Crystal Structures and Physical Properties of Bis(ethylenedithio)-tetrathiafulvalene Charge-transfer Salts with FeX_4^- (X = Cl or Br) Anions†

Talal Mallah, Claire Hollis, Simon Bott, Mohamedally Kurmoo, and Peter Day*
Inorganic Chemistry Laboratory, Oxford University, South Parks Road, Oxford OX1 3QR
Margaret Allan and Richard H. Friend
Cavendish Laboratory, Madingley Road, Cambridge CB3 0HE

Two new charge-transfer salts $[bettf]_2[FeCl_4]$ (**1**) and $[bettf][FeBr_4]$ (**2**) have been prepared and crystallised electrochemically [bettf = bis(ethylenedithio)tetrathiafulvalene]. The crystal structures of both salts have been refined in the $P\bar{1}$ space group, the unit-cell parameters being: (**1**), a = 6.626(2), b = 15.025(2), c = 17.805(2), α = 82.80(2), β = 89.53(2), γ = 88.15(2), Z = 2, R = 0.044; (**2**), a = 8.634(2), b = 10.980(2), c = 11.773(2), Å, α = 91.91(2), β = 102.84(2), γ = 93.73(2), Z = 2, R = 0.054. The structure of (**1**) consists of stacks of dimerised bettf molecules with short S • • • S contacts, forming layers separated by sheets of $FeCl_4^-$. In (**2**) there are no stacks of bettf molecules: the structure consists of discrete dimers separated by $FeBr_4^-$. Compound (**1**) shows semi-conducting behaviour from 160 to 300 K with ε_a = 0.21 eV and $\sigma \approx 10^{-2}$ S cm^{-1} at 300 K while (**2**) is a quasi-insulator at room temperature with $\sigma \approx 10^{-6}$ S cm^{-1}. The magnetic susceptibility of both salts from 5 to 300 K is dominated by the $S = \frac{5}{2}$ Fe^{3+} with small Weiss constants [$-6(1)$ for (**1**) and $-5(1)$K for (**2**)].

The last few years have seen the synthesis of numerous charge-transfer salts of the S-heterocyclic molecule bis(ethylenedithio)tetrathiafulvalene (bettf), following the discovery of superconductivity, first under pressure in $[bettf]_2[ReO_4]$ (T_c 2 K, $P \approx$ 4.5 kbar)[1] and later at ambient pressure in β-$[bettf]_2[I_3]$-(T_c 1.4K).[2] These efforts culminated recently in the preparation of κ-$[bettf]_2[Cu(NCS)_2]$ with the highest superconducting critical temperatures yet found in a molecular solid (10.4K).[3] One aspect of the potential flexibility of structures in this class of compound that has not received much attention so far[4] is the incorporation of anions carrying a magnetic moment, although the interplay of magnetism and superconductivity is a recurring theme in the theory of classical superconductors. For this reason, as part of our extended programme on the relationship between structure and physical properties in bettf salts, we have synthesised compounds containing transition elements within the anions. In this paper we report the preparation, crystal structures, conductivity, and magnetic susceptibility of bettf salts of FeX_4^- (X = Cl or Br). Comparisons can be made between these compounds and those containing non-magnetic anions such as GaI_4^-[5] and $InBr_4^-$.[6]

Experimental

Synthesis and Crystal Growth.—The compound bettf was prepared by the literature method.[7] Tetraethylammonium salts of the anions FeX_4^- (X = Cl or Br) were prepared by treating the metal halide with ammonium halides in ethanolic solution. The resulting precipitates were recrystallised from hot ethanol. All products had satisfactory elemental analyses. Electrocrystallisation was carried out in a three-compartment H-shaped cell consisting of an anode separated from the cathode cell by two porous frits, which minimise the influence of unwanted side reactions of reduced species generated at the cathode. All solvents used [CH_2Cl_2, CH_3CN, and tetrahydrofuran (thf); h.p. l.c. Grade] were dried by passing through an alumina column prior to use. The use of CH_2Cl_2 alone as a solvent in the electrocrystallisation of the $FeCl_4^-$ salt led to the formation of two crystal phases while a CH_2Cl_2—CH_3CN (2:1) solvent mixture resulted in only one phase. A single phase was obtained in the electrocrystallisation of the $FeBr_4^-$ salt in neat CH_2Cl_2. The concentration of tetrahalogenoferrate(III) was 1–2 mmol dm^{-3} in both cases. The platinum electrodes were soaked in *aqua regia*, rinsed in deionised water, then acetone, and dried at 120 °C. The cells were cleaned by the same sequence of solvents.

Crystal growth was carried out under galvanostatic conditions. Current levels greater than 10 µA resulted in very rapid crystal growth and produced microcrystals or powder, whereas for low current levels (< 1 µA), side reactions and diffusion from the electrode competed with nucleation at the electrode and led to poor-quality crystals and low yields. The optimum current was determined by initially setting it to a low value and then increasing it by 1µA every 24 h until crystal growth began at the anode, after which a constant current was maintained until all the bettf had been used. The crystals of $[bettf]_2[FeCl_4]$ (**1**) were long, thin, black needles and those of $[bettf][FeBr_4]$ (**2**) were black and rod-shaped. Both had a metallic lustre.

Determination of the Crystal Structures.—Data were collected on crystals whose quality had been checked by Laue photographs using an Enraf-Nonius CAD4 automatic diffractometer. Rotation photographs confirmed that the crystals were suitable for data collection. The crystals were indexed and orientation matrices calculated using 24 reflections from a search routine. Reflections were collected by ω—2θ scans over a 2θ range 0—52° for (**1**) and 0—52° for (**2**) (scan widths 1.0 + 0.35 tanθ and 0.9 + 0.5tanθ respectively) using graphite-monochromated Mo-K_α radiation, of which 2 744 were considered unique and observed [$F \geqslant 3\sigma(F)$], R(merge) = 0.047, for (**1**) and 2 168 [R(merge) = 0.039] for (**2**). These were corrected for Lorentz and polarisation effects and an

---

* *Present address:* Institut Laue-Langevin, 156X, 38042 Grenoble, France.

† Tetrathiafulvalene = 2-(1′,3′-dithiol-2′-ylidene)-1,3-dithiole.

Non-S.I. units employed: bar = 10^5 Pa, eV $\approx 1.6 \times 10^{-19}$ J.

Supplementary data available: see Instructions for Authors, *J. Chem. Soc., Dalton Trans.*, 1990, Issue 1, pp. xix—xxii.

Table 1. Positional parameters for $[\mathrm{bettf}]_2[\mathrm{FeCl}_4]$ (fractional co-ordinates × 10^4)

Atom	*X/a*	*Y/b*	*Z/c*	Atom	*X/a*	*Y/b*	*Z/c*
Fe	234(2)	2 487(1)	5 017.6(8)	C(1)	5 850(19)	7 761(12)	2 764(7)
Cl(1)	−1 678(5)	1 888(3)	5 929(2)	C(2)	7 742(18)	7 854(13)	2 567(7)
Cl(2)	2 290(5)	1 466(2)	4 650(2)	C(3)	6 652(13)	8 271(6)	1 102(5)
Cl(3)	−1 662(5)	3 070(3)	4 081(2)	C(4)	4 713(12)	8 336(6)	1 307(5)
Cl(4)	2 061(6)	3 519(2)	5 415(2)	C(5)	4 769(13)	8 891(6)	−115(5)
S(1)	3 677(4)	8 103(2)	2 218(1)	C(6)	4 225(13)	9 150(6)	−849(5)
S(2)	8 750(4)	7 909(2)	1 655(2)	C(7)	4 283(13)	9 551(6)	−2 297(5)
S(3)	7 237(4)	8 639(2)	155(1)	C(8)	2 323(14)	9 546(6)	−2 105(5)
S(4)	2 985(4)	8 745(2)	609(1)	C(9)	1 241(19)	9 775(12)	−3 596(7)
S(5)	6 019(3)	9 314(2)	−1 565(1)	C(10)	3 174(19)	9 438(12)	−3 741(7)
S(6)	1 746(4)	9 313(2)	−1 144(1)	C(11)	6 300(18)	4 643(11)	6 159(6)
S(7)	231(4)	9 762(2)	−2 690(2)	C(12)	8 335(18)	4 832(10)	6 369(7)
S(8)	5 278(4)	9 707(2)	−3 210(1)	C(13)	7 168(14)	4 347(7)	7 824(5)
S(9)	4 238(4)	4 962(2)	6 767(2)	C(14)	5 258(14)	4 595(6)	7 662(5)
S(10)	9 238(5)	4 284(3)	7 225(2)	C(15)	5 268(13)	4 123(6)	9 095(5)
S(11)	7 713(4)	4 004(2)	8 780(1)	C(16)	4 716(13)	3 893(6)	9 832(5)
S(12)	3 520(4)	4 538(2)	8 404(1)	C(17)	4 723(14)	3 316(6)	11 257(5)
S(13)	6 469(4)	3 485(2)	10 518(1)	C(18)	2 797(14)	3 531(7)	11 094(5)
S(14)	2 233(4)	3 959(2)	10 151(1)	C(19)	1 641(18)	2 680(9)	12 439(7)
S(15)	709(4)	3 472(3)	11 697(2)	C(20)	3 607(17)	2 880(9)	12 755(6)
S(16)	5 769(4)	2 890(2)	12 133(1)				

empirical absorption correction was applied [minimum and maximum corrections: 1.00 and 1.15 for (**1**) and 1.2 and 1.4 for (**2**)]. The space group was $P\bar{1}$ in each case, which, combined with the values of the density, molecular weight, and unit-cell volumes, indicated two formula units per unit cell in each compound.

Crystal data. $\mathrm{C_{20}H_{16}Cl_4FeS_{16}}$, (**1**), $M_r = 967$, triclinic, space group $P\bar{1}$, $a = 6.626(2)$, $b = 15.025(2)$, $c = 17.805(2)$ Å, $\alpha = 82.80(2)$, $\beta = 89.53(2)$, $\gamma = 88.15(2)°$, $U = 1\,757.5$ Å^3, $Z = 2$, $D_c = 1.834$ g cm^{-3}, Mo-K_α radiation ($\lambda = 0.710\,69$ Å), 4 530 independent reflections, $R = 0.044$.

$\mathrm{C_{10}H_8Br_4FeS_8}$, (**2**), $M_r = 760$, triclinic, space group $P\bar{1}$, $a = 8.634(2)$, $b = 10.980(2)$, $c = 11.773(2)$ Å, $\alpha = 91.91(2)$, $\beta = 102.84(2)$, $\gamma = 93.73(2)°$, $U = 1\,084.5$ Å^3, $Z = 2$, $D_c = 2.33$ g cm^{-3}, Mo-K_α radiation ($\lambda = 0.710\,69$ Å), 5 986 independent reflections, $R = 0.054$.

The structures were solved by routine direct and Fourier methods using the SHELXS program.[8] It was possible to assign the Fe, Cl, and S in compound (**1**) but only 18 C. The remaining two carbon atoms were found from a difference map. Full-matrix least-squares refinement of the non-hydrogen atoms converged at R 0.130. Inclusion of anisotropic thermal parameters for Fe, Cl, and S resulted in an R value of 0.060. Further inclusion of anisotropic thermal parameters for the carbons gave R 0.048. The hydrogen atoms were generated geometrically but not refined. Following further refinements the model converged at $R = 0.044$, $R' = 0.050$.

In the case of compound (**2**) it was immediately possible to assign all non-hydrogen atoms which were refined by the full-matrix least-squares method. Initially only the positional and isotropic thermal parameters of the Fe, Br, and S atoms were refined, while later refinements included the parameters relating to the C atoms, to give R 0.140. After including anisotropic thermal parameters for all atoms, a difference map readily revealed the positions of some of the hydrogen atoms and the rest were generated geometrically. The latter were included in the list but not refined. Following further refinements and the application of the Chebyshev weighting scheme[9] the model converged at $R = 0.054$, $R' = 0.062$.

Additional material available from the Cambridge Crystallographic Data Centre comprises thermal parameters.

Electrical Conductivity.—Conductivities of single crystals were measured from 160 to 300 K by the two-probe d.c. method using silver paint as electrical contact.

Magnetic Susceptibility.—The temperature dependence of the magnetic susceptibility of samples consisting of randomly oriented microcrystals was measured by the Faraday method from 5 to 300 K. In each case the samples came from a single batch, checked for homogeneity by microscopic examination of the crystal morphology. The crystals used for the structure determinations were selected from the same batches. Honda-Owen[10] corrections were made for small fractions of ferromagnetic impurities [fitted as 270 p.p.m. of iron for (**1**) and 25 p.p.m. for (**2**)]. Diamagnetic corrections of 301×10^{-6} for (**1**) and 341×10^{-6} e.m.u. mol^{-1} for (**2**) were also applied to the data (e.m.u. = S.I × $10^6/4\pi$).

Results

Crystal Structures.—$[\mathrm{bettf}]_2[\mathrm{FeCl}_4]$ (**1**). Positional parameters of the final solution of the structure of compound (**1**) are shown in Table 1, bond lengths and angles in Table 2, and intermolecular distances less than 4.0 Å in Table 3. The asymmetric unit contains two independent bettf molecules, labelled X and Y, and one $\mathrm{FeCl_4}^-$ anion.

The structure of $[\mathrm{bettf}]_2[\mathrm{FeCl}_4]$ consists of dimerised stacks of bettf molecules separated by sheets of tetrahedral $\mathrm{FeCl_4}^-$ anions (Figure 1). The anions are situated in an 'anion cavity' formed by the ethylene groups of the bettf molecules. Within the stacks, the bettf molecules are normal to the *b*-direction and are parallel with respect to each other (Figure 2). The intrastack packing-mode alternates between the a and c modes, as defined by Williams.[11] The molecules are arranged in the sequence ···X Y Y X X Y Y X··· (Figure 1). Adjacent molecules of the same type (XX′ and YY′) have the a mode of intrastack packing [Figure 3(*a*)], *i.e.* the molecules stack uniformly on top of each other but with a slight displacement between neighbours along the long in-plane molecular axis. On the other hand, adjacent molecules of different type (XY′ and YX′) have the c mode of stacking [Figure 3(*b*)] in which the long in-plane molecular axes along a column are rotated relative to one another. This arrangement of the bettf molecules also leads to a slight dimerisation within the stacks; the related bettf molecules X and

Table 2. Bond lengths (Å) and angles (°) for $[\text{bettf}]_2[\text{FeCl}_4]$

Cation 1				Cation 2			
S(1)–C(1)	1.77(1)	S(1)–C(4)	1.755(9)	S(9)–C(11)	1.83(1)	S(9)–C(14)	1.753(9)
S(2)–C(2)	1.74(1)	S(2)–C(3)	1.743(9)	S(10)–C(12)	1.74(1)	S(10)–C(13)	1.738(9)
S(3)–C(3)	1.751(9)	S(3)–C(5)	1.725(9)	S(11)–C(13)	1.751(9)	S(11)–C(15)	1.721(9)
S(4)–C(4)	1.739(9)	S(4)–C(5)	1.740(9)	S(12)–C(14)	1.741(9)	S(12)–C(15)	1.741(9)
S(5)–C(6)	1.735(8)	S(5)–C(7)	1.741(9)	S(13)–C(16)	1.734(9)	S(13)–C(17)	1.745(9)
S(6)–C(6)	1.729(9)	S(6)–C(8)	1.745(9)	S(14)–C(16)	1.740(9)	S(14)–C(18)	1.76(1)
S(7)–C(8)	1.738(9)	S(7)–C(9)	1.74(1)	S(15)–C(18)	1.74(1)	S(15)–C(19)	1.76(1)
S(8)–C(7)	1.741(9)	S(8)–C(10)	1.78(1)	S(16)–C(17)	1.75(1)	S(16)–C(20)	1.80(1)
C(1)–C(2)	1.31(2)	C(3)–C(4)	1.34(1)	C(11)–C(12)	1.45(2)	C(13)–C(14)	1.33(1)
C(5)–C(6)	1.36(1)	C(7)–C(8)	1.34(1)	C(15)–C(16)	1.36(1)	C(17)–C(18)	1.33(1)
C(10)–C(9)	1.40(2)			C(19)–C(20)	1.48(2)		
C(4)–S(1)–C(1)	101.7(5)	C(3)–S(2)–C(2)	101.7(5)	C(14)–S(9)–C(11)	100.5(5)	C(13)–S(10)–C(12)	102.7(5)
C(5)–S(3)–C(3)	95.1(4)	C(5)–S(4)–C(4)	95.0(4)	C(15)–S(11)–C(13)	95.5(4)	C(17)–S(13)–C(16)	95.6(4)
C(7)–S(5)–C(6)	95.5(4)	C(8)–S(6)–C(6)	95.4(4)	C(18)–S(14)–C(16)	95.0(4)	C(19)–S(15)–C(18)	100.0(5)
C(9)–S(7)–C(8)	103.5(5)	C(10)–S(8)–C(7)	100.7(5)	C(20)–S(16)–C(17)	102.3(5)	C(12)–C(11)–S(9)	117.5(9)
C(2)–C(1)–S(1)	128.0(10)	C(1)–C(2)–S(2)	127.0(10)	C(11)–C(12)–S(10)	117.1(9)	S(11)–C(13)–S(10)	113.8(5)
S(3)–C(3)–S(2)	113.9(5)	C(4)–C(3)–S(2)	129.2(7)	C(14)–C(13)–S(10)	129.8(7)	C(14)–C(13)–S(11)	116.4(7)
C(4)–C(3)–S(3)	116.9(7)	S(4)–C(4)–S(1)	114.7(5)	S(12)–C(14)–S(9)	114.7(5)	C(13)–C(14)–S(9)	127.3(7)
C(3)–C(4)–S(1)	127.8(7)	S(4)–C(5)–S(3)	115.4(5)	S(12)–C(15)–S(11)	115.4(5)	C(16)–C(15)–S(11)	122.7(7)
C(6)–C(5)–S(3)	122.8(7)	C(6)–C(5)–S(4)	121.7(7)	C(16)–C(15)–S(12)	121.9(7)	S(14)–C(16)–S(13)	115.1(5)
S(6)–C(6)–S(5)	115.1(5)	C(5)–C(6)–S(5)	121.4(7)	C(15)–C(16)–S(14)	123.3(7)	S(16)–C(17)–S(13)	114.5(5)
C(5)–C(6)–S(6)	123.5(7)	S(8)–C(7)–S(5)	116.3(5)	C(18)–C(17)–S(13)	117.3(7)	C(18)–C(17)–S(16)	128.2(7)
C(8)–C(7)–S(5)	117.0(7)	C(8)–C(7)–S(8)	126.6(7)	S(15)–C(18)–S(14)	114.0(6)	C(17)–C(18)–S(14)	117.1(7)
S(7)–C(8)–S(6)	114.5(5)	C(7)–C(8)–S(6)	117.0(7)	C(20)–C(19)–S(15)	115.7(9)	C(19)–C(20)–S(16)	117.2(8)
C(7)–C(8)–S(7)	128.5(7)	C(9)–C(10)–S(8)	120.6(11)				
C(10)–C(9)–S(7)	123.5(10)						
Anion							
Fe–Cl(1)	2.174(3)	Fe–Cl(2)	2.177(3)	Cl(2)–Fe–Cl(1)	109.7(1)	Cl(3)–Fe–Cl(1)	109.0(1)
Fe–Cl(3)	2.174(3)	Fe–Cl(4)	2.186(4)	Cl(3)–Fe–Cl(2)	110.1(2)	Cl(4)–Fe–Cl(2)	110.1(2)
				Cl(4)–Fe–Cl(1)	107.7(2)	Cl(4)–Fe–Cl(2)	110.2(2)

X′ (or Y and Y′) are closer to each other ($\approx$3.60 Å) than the two independent ones X and Y (3.81 Å).

The shortest distances between bettf molecules in compound (**1**) are observed between the stacks in the *a*-direction [*e.g.* S(1)$\cdots$S(2) 3.455, S(6)$\cdots$S(8) 3.423; S(5)$\cdots$S(7) 3.457, S(15)$\cdots$S(16) 3.472, and S(13)$\cdots$S(15) 3.519 Å]. These distances are shorter than the sum of the van der Waals radii of two sulphur atoms (d = 3.60 Å), thus suggesting the possibility of a quasi-one-dimensional interaction along the *a* direction.

$[\text{bettf}][\text{FeBr}_4]$ (**2**). Final positional parameters for compound (**2**) are shown in Table 4, bond lengths and angles in Table 5, and intermolecular distances less than 4.0 Å in Table 6. The asymmetric unit contains one bettf molecule and one FeBr_4^- anion (Figure 4). Compound (**2**) is the third 1:1 bettf charge-transfer salt observed to date, the others being $[\text{bettf}][\text{ReO}_4]\cdot 0.5$ thf and $[\text{bettf}][\text{IO}_4]\cdot 0.5$ thf.

The main feature of the structure of $[\text{bettf}][\text{FeBr}_4]$ is the absence of stacks and planes of closely spaced bettf, in marked contrast to most bettf compounds. Intradimer overlap is of the a type, but there are no S$\cdots$S distances within each dimer shorter than the combined van der Waals radii of two sulphur atoms (3.60 Å), the shortest being 3.72 Å, which indicates the absence of any intradimer interaction. The only short S$\cdots$S distances ($<$3.50 Å) are between two bettf molecules in different pairs, as shown in Figures 2 and 3, but there is no continuous network of short S$\cdots$S contacts through the lattice.

The FeBr_4^- anions form a three-dimensional lattice separated by pairs of bettf molecules (Figure 5). One FeBr_4^- ion has short intermolecular distances to two bettf molecules but this is isolated from any other short interactions so that no long-range interaction between bettf molecules through the FeBr_4^- anions is possible, which correlates with the insulating behaviour of this compound.

Electrical Conductivity.—From 160 to 300 K the conductivity of compound (**1**) follows a simple semiconducting activation law, with an activation energy ε_a = 0.21 eV and a specific conductivity of 10^{-2} S cm^{-1} at 300 K. There was no evidence for any discontinuities in the conductivity or changes of activation energy over this temperature range, such as have been found in some other semiconducting bettf salts like α-$[\text{bettf}]_2[\text{AuBr}_2]$[13] and $[\text{bettf}]_2[\text{CF}_3\text{SO}_3]$.[14] Below 160 K the resistance of the crystals became too high to measure. Compound (**2**) has a much lower conductivity than (**1**) (10^{-6} S cm^{-1} at 300 K) so that its temperature dependence could not be measured to determine an activation energy.

Magnetic Susceptibility.—After applying the corrections for diamagnetism and ferromagnetic impurities, the excess molar susceptibilities of the two compounds were fitted to the Curie–Weiss law $\chi = \chi_0 + C/(T - \theta)$. Excellent fits were obtained over the whole temperature range from 5 to 300 K. The values of the parameters were as follows: (**1**), C 4.7(3), χ_0 0(5) $\times$ 10^{-4} e.m.u. mol^{-1}, $\theta = -6(1)$K; (**2**), C, 4.4(1), χ_0 0(8) $\times$ 10^{-4} e.m.u. mol^{-1}, $\theta = -5(1)$ K. From the values of C one can estimate the magnetic moment per molecule as 6.1(1) μ_B for (**1**) and 5.9(1) μ_B for (**2**). These moments are close to that expected for an $S = \frac{5}{2}$ ion with an orbital singlet ground state (5.92 μ_B) as required for high-spin $3d^5\text{Fe}^{3+}$, and show that the magnetic properties are dominated by the anions. In particular, the quality of the fits of the susceptibility to a simple Curie–Weiss temperature dependence from 5 to 300 K suggests that there is no detectable contribution from interacting moments on the cations.

Discussion

Structurally and electronically, the most striking feature of the

Table 3. Intermolecular S ··· S distances in $[bettf]_2[FeCl_4]$ less than 4 Å

Cation 1–cation 1			
$x-1, y, z$			
S(1) ··· S(2)	3.455	S(6) ··· S(8)	3.423
$1-x, 2-y, -z$			
S(1) ··· S(5)	3.920		
S(3) ··· S(4)	3.992	S(3) ··· S(6)	3.813
$1+x, y, z$			
S(2) ··· S(4)	3.533	S(3) ··· S(4)	3.912
S(3) ··· S(6)	3.846	S(5) ··· S(6)	3.874
S(5) ··· S(7)	3.457		
Cation–cation 2			
$1-x, 1-y, 1-z$			
S(1) ··· S(11)	3.957	S(5) ··· S(16)	3.809
$2-x, 1-y, 1-z$			
S(2) ··· S(10)	3.837	S(2) ··· S(11)	3.800
Cation 2–cation 2			
$x-1, y, z$			
S(9) ··· S(10)	3.556	S(15) ··· S(16)	3.472
$1-x, 1-y, 2-z$			
S(9) ··· S(16)	3.979	S(11) ··· S(15)	3.953
S(11) ··· S(14)	3.803	S(12) ··· S(13)	3.734
S(12) ··· S(16)	3.906	S(13) ··· S(14)	3.995
$1+x, y, z$			
S(11) ··· S(12)	3.990	S(11) ··· S(14)	3.873
S(13) ··· S(15)	3.519		
Anion–cation 1			
$-x, 1-y, 1-z$		$1-x, 1-y, -z$	
Cl(1) ··· S(1)	3.546	Cl(2) ··· S(8)	3.627
$x, y-1, 1-z$			
Cl(1) ··· S(7)	3.958		
Anion–cation 2			
$x-1, y, z-1$			
Cl(3) ··· S(16)	3.919		
$x-1, y, z$		$-x, 1-y, 1-z$	
Cl(4) ··· S(10)	3.987	Cl(3) ··· S(9)	3.540

Table 4. Positional parameters for $[bettf][FeBr_4]$ (fractional co-ordinates × 10^4)

Atom	*X/a*	*Y/b*	*Z/c*
Fe	4 307(3)	1 967(2)	7 247(2)
Br(1)	4 014(2)	1 829(2)	9 160(1)
Br(2)	6 250(2)	700(1)	6 958(2)
Br(3)	1 903(2)	1 345(2)	5 966(1)
Br(4)	5 098(3)	3 959(1)	6 887(2)
S(1)	−1 555(4)	1 063(3)	536(3)
S(2)	1 683(4)	2 323(3)	2 729(3)
S(3)	−474(4)	2 957(3)	−877(3)
S(4)	2 218(4)	3 967(3)	932(3)
S(5)	3 196(4)	5 849(3)	−896(3)
S(6)	491(5)	4 808(3)	−2 675(3)
S(7)	4 268(5)	7 661(3)	−2 416(3)
S(8)	1 014(16)	6 399(3)	−4 518(3)
C(1)	−351(18)	316(11)	1 722(12)
C(2)	200(16)	1 112(12)	2 826(11)
C(3)	1 104(16)	2 737(11)	1 319(10)
C(4)	−159(15)	2 281(10)	456(10)
C(5)	1 096(15)	4 033(10)	−463(10)
C(6)	1 544(15)	4 816(10)	−1 248(10)
C(7)	2 910(16)	6 479(9)	−2 239(10)
C(8)	1 622(15)	5 995(10)	−3 097(10)
C(9)	4 105(21)	7 468(14)	−3 972(13)
C(10)	2 521(25)	7 509(16)	−4 700(15)

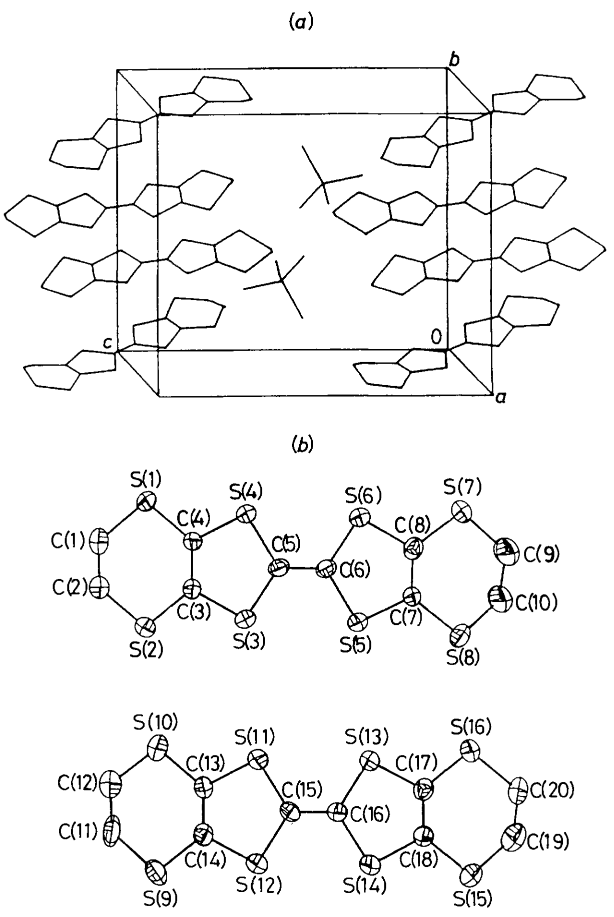

Figure 1. (*a*) The XXYYXX stacking sequence of bettf molecules in $[bettf]_2[FeCl_4]$. (*b*) Atom numbering of the independent bettf

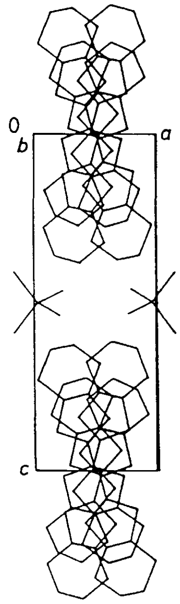

Figure 2. A projection of the unit cell of $[bettf]_2[FeCl_4]$ along the *b* axis

two FeX_4^- salts of bettf is that they have different chemical stoicheiometries, and hence band fillings. The structure of (**1**) is closely related to those of $[bettf]_2[InBr_4]$,[6] α-$[bettf]_2[PF_6]$,[15] β-$[bettf]_2[PF_6]$,[16] and $[bettf]_2[AsF_6]$.[17] In the case of $[bettf]_2[InBr_4]$ the intrastack distances (X ··· X′ 3.43, X ··· Y 3.87, and Y ··· Y′ 3.47 Å) are shorter than those found in $[bettf]_2[FeCl_4]$, indicating a greater degree of intrastack dimerisation, whilst the interstack distances are greater

Table 5. Bond lengths (Å) and angles (°) for [bettf][FeBr$_4$]

Cation			
S(1)–C(1)	1.802(14)	S(1)–C(4)	1.761(12)
S(2)–C(2)	1.810(13)	S(2)–C(3)	1.710(12)
S(3)–C(4)	1.733(11)	S(3)–C(5)	1.712(12)
S(4)–C(3)	1.739(13)	S(4)–C(5)	1.718(13)
S(5)–C(6)	1.729(13)	S(5)–C(7)	1.721(11)
S(6)–C(6)	1.723(12)	S(6)–C(8)	1.733(12)
S(7)–C(7)	1.741(13)	S(7)–C(9)	1.809(14)
S(8)–C(8)	1.720(12)	S(8)–C(10)	1.777(18)
C(1)–C(2)	1.508(19)	C(3)–C(4)	1.369(17)
C(5)–C(6)	1.383(15)	C(7)–C(8)	1.388(18)
C(9)–C(10)	1.448(24)		
C(1)–S(1)–C(4)	97.57(63)	C(2)–S(2)–C(3)	102.95(63)
C(4)–S(3)–C(5)	98.84(58)	C(3)–S(4)–C(4)	96.22(56)
C(6)–S(5)–C(7)	95.86(62)	C(6)–S(6)–C(8)	96.62(60)
C(7)–S(7)–C(9)	99.53(69)	C(8)–S(8)–C(10)	104.18(75)
S(1)–C(1)–C(2)	114.00(85)	S(2)–C(2)–C(1)	113.72(91)
S(2)–C(3)–S(4)	115.73(77)	S(2)–C(3)–C(4)	129.62(97)
S(4)–C(3)–C(4)	114.57(84)	S(1)–C(4)–S(3)	114.48(70)
S(3)–C(5)–S(4)	116.15(62)	S(3)–C(5)–C(6)	121.67(94)
S(4)–C(5)–C(6)	121.76(93)	S(5)–C(6)–S(6)	115.06(68)
S(5)–C(6)–C(5)	123.37(93)	S(6)–C(6)–S(6)	121.56(95)
S(5)–C(7)–S(7)	117.43(78)	S(5)–C(7)–C(8)	117.31(88)
S(7)–C(7)–C(8)	125.25(87)	S(6)–C(8)–S(8)	115.83(73)
S(6)–C(8)–C(7)	115.04(85)	S(8)–C(8)–C(7)	129.13(90)
S(7)–C(9)–C(10)	115.93(120)	S(8)–C(10)–C(9)	118.30(119)
Anion			
Fe–Br(1)	2.330(2)	Fe–Br(2)	2.322(2)
Fe–Br(3)	2.325(3)	Fe–Br(4)	2.330(2)
Br(1)–Fe–Br(2)	108.81(10)	Br(1)–Fe–Br(3)	109.45(10)
Br(1)–Fe–Br(4)	111.01(10)	Br(2)–Fe–Br(3)	109.54(11)
Br(2)–Fe–Br(4)	108.46(10)	Br(3)–Fe–Br(4)	109.54(10)

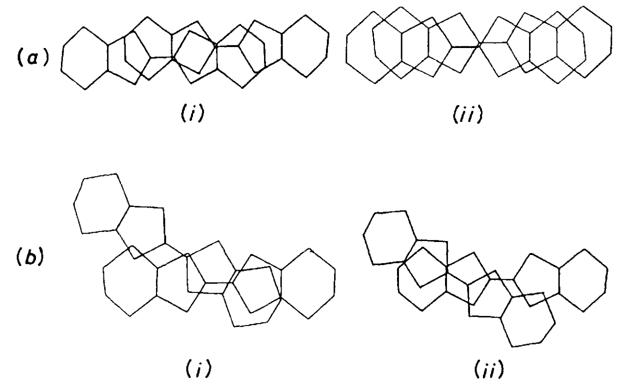

Figure 3. Modes of stacking in [bettf]$_2$[FeCl$_4$]. (a) Between molecules of the same type: (i) X and X′, (ii) Y and Y′. (b) Between molecules of different types: (i) X and Y′; (ii) Y and X′

Table 6. Intermolecular distances (Å) in [bettf][FeBr$_4$]

Cation–cation			
$-x, 1-y, -z$			
S(1) • • • S(5)	3.806	S(1) • • • S(7)	3.857
S(2) • • • S(8)	3.772	S(2) • • • S(6)	3.769
S(3) • • • S(4)	3.783	S(3) • • • S(5)	3.741
S(4) • • • S(6)	3.724		
$1-x, 1-y, -z$			
S(2) • • • S(7)	3.595	S(4) • • • S(7)	3.743
S(4) • • • S(5)	3.961	S(5) • • • S(5)	3.965
$-x, 1-y, -1-z$			
S(6) • • • S(8)	3.454	S(8) • • • S(8)	3.461
Cation–anion			
$1+x, y, 1+x$			
Br(1) • • • S(1)	3.965		
$x, y, 1+z$			
Br(1) • • • S(4)	3.722	Br(4) • • • S(5)	3.974
$1-x, -y, 1-z$			
Br(2) • • • S(2)	3.861		
$-x, -y, 1-z$			
Br(1) • • • S(1)	3.776	Br(3) • • • S(2)	3.656
$1-x, 1-y, 1-z$			
Br(1) • • • S(5)	3.625	Br(1) • • • S(7)	3.799
Br(4) • • • S(4)	3.664		
$1-x, 1-y, -z$			
Br(2) • • • S(7)	3.820		
x, y, z			
Br(3) • • • S(2)	3.961		
$-x, 1-y, -z$			
Br(3) • • • S(8)	3.817		

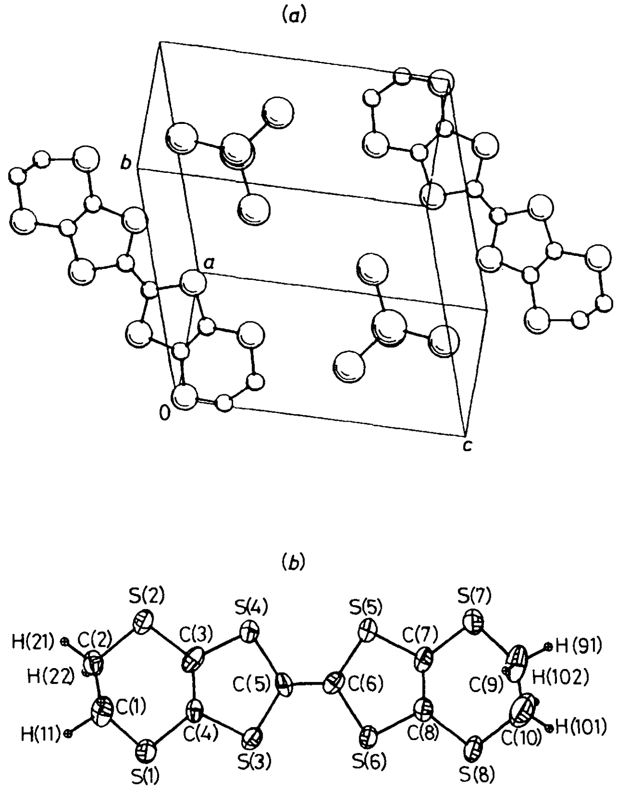

Figure 4. (a) The unit cell of [bettf][FeBr$_4$]. (b) Atom numbering of bettf

($d > 3.55$ Å). This is probably due to the greater size of the InBr$_4$$^-$ anion. However, the structure of salts containing octahedral anions, α- and β-[bettf]$_2$[PF$_6$] and [bettf]$_2$[AsF$_6$], exhibit interstack side-by-side contact distances nearly identical to those found in [bettf]$_2$[FeCl$_4$].

As is the case for [bettf]$_2$[FeCl$_4$], no short contact distances between sulphur atoms are observed in the PF$_6$ and AsF$_6$ compounds along the molecular stacking direction and so their conduction properties are highly one-dimensional. For example, conductivity measurements on β-[bettf]$_2$[PF$_6$] have shown that the ratio of the conductivities along the direction of side-by-side contacts to that along the molecular stacking direction is 200 : 1.[15,16] Our single-crystal conductivity measurements show that [bettf]$_2$[FeCl$_4$] is also semi-conducting, like the PF$_6$ and AsF$_6$ salts, with an activation energy of

Table 7. Volume of unit cell (V_{cell}) and anion (V_{anion}) in [bettf]$_2$X salts with tetrahedral anions X

Salt	V_{cell}/Å^3	V_{anion}/Å^3	Ref.
[bettf]$_2$[ReO$_4$]	1 565	157	18
[bettf]$_2$[BrO$_4$]	1 589	136	18
[bettf]$_2$[FeCl$_4$]	1 758	272	This work
[bettf]$_2$[InBr$_4$]	1 820	370	6
[bettf]$_2$[AsF$_6$]	3 274	111	17

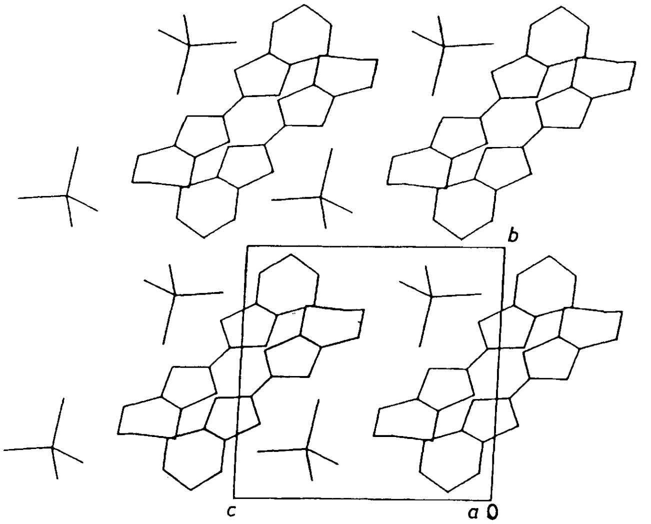

Figure 5. Projection of the unit cell of [bettf][FeBr$_4$] along *a*, showing the presence of dimers

0.21 eV, but because of the needle-like crystal habit we have no information on the anisotropy.

There are several possible origins for the tendency towards a side-by-side packing arrangement of the bettf in these three compounds: (*i*) as the atoms of the ethylene groups are not on the molecular plane, intermolecular steric repulsions make the more normal face-to-face overlap unstable; (*ii*) in π-donor molecules with chalcogen atoms, face-to-face overlap may not in fact be necessary for significant intermolecular interaction since a mixing of the p_π and d_π orbitals can be expected. A side-by-side arrangement is not suitable for p_π–p_π interaction but it is not unfavourable for d_π–d_π interaction.

The structure of compound (**1**) contrasts with the structures of bettf salts with tetrahedral oxyanions such as [bettf]$_2$[ReO$_4$] and [bettf]$_2$[BrO$_4$],[18] which have a zigzag arrangement of bettf molecules along the *a* direction that allows the formation of a 'corrugated sheet' network with intermolecular separations less than 3.60 Å. The two-dimensional nature of the latter structure is reflected in the conductivities of the ReO$_4$ and BrO$_4$ salts. Thus, [bettf]$_2$[ReO$_4$] is metallic at room temperature and is a superconductor at 2 K under a pressure of 5 kbar[1].

The unit cell and anion volumes of some related bettf salts of tetrahedral anions are listed in Table 7. The volumes of the anions were estimated as those of spheres with radii equal to the observed M–X bond length of MX$_n^-$ plus the radius of X. The large volumes of FeCl$_4^-$ and InBr$_4^-$ lead to a bigger unit cell and therefore to a greater intermolecular separation between the bettf.

Molecular orbital calculations[19] have shown that increasing the positive charge on the bettf molecule results in an increase in the distance between the two carbon atoms in the centre of the molecule and a decrease in the C–S bond lengths. Both of the crystallographically independent bettf molecules in [bettf]$_2$[FeCl$_4$] have a C=C bond length of 1.36 Å, indicating that they are essentially identical and that the formal charge on each is $+\frac{1}{2}$. The intramolecular bond lengths of the bettf in some other [bettf]$_n$X$_m$ charge-transfer salts are shown in Table 8, from which the bond lengths of those compounds, in which the molecules carry a formal positive charge of $+\frac{1}{2}$, can be seen to be very similar to the corresponding bond lengths in [bettf]$_2$[FeCl$_4$].

Table 8. Some bond lengths (Å) within the bettf molecules in salts of different stoicheiometry (d_1 is the central C=C double bond; d_2 the C–S bond nearest the molecular centre, d_3 the other C–S bond, and d_4 the outer C=C bond)

Compound	Charge	d_1	d_2	d_3	d_4
bettf	0	1.32	1.76	1.75	1.33
β-[bettf]$_2$I$_3$	$+\frac{1}{2}$	1.35	1.74	1.76	1.34
[bettf]$_2$[FeCl$_4$]:					
Cation 1	$+\frac{1}{2}$	1.360	1.732	1.744	1.340
Cation 2	$+\frac{1}{2}$	1.360	1.734	1.749	1.330
γ-[bettf]$_3$[ClO$_4$]$_2$	$+\frac{2}{3}$	1.37	1.73	1.74	1.34
[bettf][ReO$_4$]·0.5 thf	+1	1.38	1.72	1.73	1.37
[bettf][FeBr$_4$]	+1	1.38	1.72	1.73	1.38

Given that the formal charge per bettf molecule is $+\frac{1}{2}$, a contribution to the susceptibility from unpaired spins on the cations would be expected. For example, [bettf]$_2$[GaCl$_4$] has a temperature-dependent excess molar susceptibility with a broad maximum near 90 K of $\chi_{max.} = 1.6 \times 10^{-3}$ e.m.u. mol^{-1}, which can be fitted over the temperature range 70—300 K by either a one-dimensional (Bonner–Fisher) or quadratic layer antiferromagnetic model[20] to yield values of the exchange parameter *J* of respectively 66.5(5) and 89.6(1) K. These values of $\chi_{max.}$ and *J* are of similar magnitude to those found for the semiconducting α′-[bettf]$_2$X with X = AuBr$_2$, Ag(CN)$_2$, or CuCl$_2$[21], where the absolute value of the susceptibility was in good agreement with that expected for localised moments corresponding to $S = \frac{1}{2}$ per pair of bettf. Unfortunately, in the FeCl$_4^-$ salt, the susceptibility is dominated by the anion so that, for example, $\chi = 4.76 \times 10^{-2}$ e.m.u. mol^{-1} at 90 K, about 30 times larger than $\chi_{max.}$ for the GaCl$_4^-$ salt. Thus the magnetic properties of the cation sublattice are obscured by those of the anions. Nevertheless, it remains of interest that the Weiss constant is small (−6K), indicating only weak antiferromagnetic interaction between the anions.

In [bettf][FeBr$_4$], on the other hand, the bettf molecules are fully oxidised, each having a formal positive charge of +1. Extended-Hückel calculations[19] have characterised the highest occupied molecular orbital of bettf as bonding with respect to the C=C bonds, and antibonding with respect to the C–S bonds. Thus, loss of an electron from this molecular orbital diminishes the bonding character of the C=C bond (which results in a lengthening of the bond) and the antibonding character of the C–S bond (resulting in a shortening of the C–S bonds). That this is indeed the case can be seen in Table 8. It is likely that the absence of stacks of cations in the structure is a result of Coulomb repulsion between the relatively large charges. That, and the stoicheiometry, lead to an insulating ground state.

As far as the magnetic properties of [bettf][FeBr$_4$] are concerned, one might anticipate a moment equivalent to $S = \frac{1}{2}$ per bettf molecule in addition to $S = \frac{5}{2}$ per FeBr$_4^-$. That the susceptibility obeys the Curie–Weiss law from 5 to 300 K with a moment equivalent to 5.9 μ_B per formula unit suggests that, as in the FeCl$_4^-$ salt, the Fe^{3+} dominates the contribution of the bettf. It is worth noting that a similar conclusion was reached in two earlier studies of charge-transfer salts containing high-spin anions, [ttf][MnCl$_4$]$_{0.25}$[22] and [bettf]$_3$[MnCl$_4$]$_2$.[23] Crystallographic evidence suggests that the latter contains one third its cations in the form of bettf$^+$, as in [bettf][FeBr$_4$].

Acknowledgements

We acknowledge the S.E.R.C. for partial support of this work, and thank Dr. D. Watkin for helpful discussions.

References

1 S. S. S. Parkin, E. M. Engler, R. R. Schumaker, R. Lagier, V. Y. Lee, J. C. Scott, and R. L. Greene, *Phys. Rev. Lett.*, 1983, **50**, 270.

2 E. B. Yagubskii, I. F. Shchegelov, V. N. Laukhin, P. A. Kononovich, M. V. Kartsovnik, A. V. Zvarykina, and L. I. Buravov, *Zh. Eksp. Teor. Fiz., Pis'ma Red.*, 1984, **39**, 12.

3 H. Urayama, H. Yamochi, G. Saito, K. Nozawa, T. Sugano, M. Kinoshita, S. Sato, K. Oshima, A. Kawamoto, and J. Tanaka, *Chem. Lett.*, 1988, 55.

4 T. Mori and H. Inokuchi, *Synth. Met.*, 1988, **27**, A451; *Bull. Chem. Soc. Jpn.*, 1988, **61**, 591.

5 U. Geiser, H. H. Wang, J. A. Schlueter, S. L. Hallenbeck, T. J. Allen, M. Y. Chen, H-C. Ivy Kao, K. D. Carlson, L. E. Gerdom, and J. M. Williams, *Acta Crystallogr., Sect. C*, 1988, **44**, 1544.

6 M. A. Beno, D. D. Cox, J. M. Williams, and J. F. Kwak, *Acta Crystallogr., Sect. C*, 1984, **40**, 1334.

7 H. H. Wang, P. E. Reed, and J. M. Williams, *Synth. Met.*, 1986, **14**, 165; M. Mizuno, A. F. Garito, and M. P. Cava, *J. Chem. Soc., Chem. Commun.*, 1978, 18.

8 G. M. Sheldrick, SHELXS 86, User Guide, University of Göttingen, 1986.

9 E. Prince, 'Mathematical Techniques in Crystallography,' Springer, New York, 1982.

10 K. Honda, *Ann. Phys.* (*Leipzig*), 1910, **32**, 1048; M. Owen, *ibid.*, 1912, **37**, 657.

11 J. M. Williams, H. H. Wang, T. J. Emge, U. Geiser, M. A. Beno, P. C. W. Leung, K. D. Carlson, R. J. Thorn, A. J. Schultz, and M. Whangbo, *Prog. Inorg. Chem.*, 1987, **35**, 51.

12 H. Kobayashi, A. Kobayashi, Y. Sasaki, G. Saito, and H. Inokuchi, *Chem. Lett.*, 1984, 183.

13 I. D. Parker, R. H. Friend, M. Kurmoo, and P. Day, *Synth. Met.*, 1988, **27**, 455; *J. Phys. Condensed Matter*, 1989, **1**, 5681.

14 D. Chasseau, D. Watkin, M. J. Rosseinsky, M. Kurmoo, D. R. Talham, and P. Day, *Synth. Met.*, 1988, **24**, 117.

15 H. Kobayashi, R. Kato, T. Mori, A. Kobayashi, Y. Sasaki, G. Saito, and H. Inokuchi, *Chem. Lett.*, 1983, 759.

16 H. Kobayashi, T. Mori, R. Kato, A. Kobayashi, Y. Sasaki, G. Saito, and H. Inokuchi, *Chem. Lett.*, 1983, 581.

17 P. C. W. Leung, M. A. Beno, G. S. Blackman, B. R. Coughlin, C. A. Miderski, W. Joss, G. W. Crabtree, and J. M. Williams, *Acta Crystallogr., Sect. C*, 1984, **40**, 1331.

18 J. M. Williams, M. A. Beno, H. H. Wang, P. E. Reed, L. J. Azevedo, and J. E. Schirber, *Inorg. Chem.*, 1984, **23**, 1790.

19 T. Mori, A. Kobayashi, Y. Sasaki, H. Kobayashi, G. Saito, and H. Inokuchi, *Bull. Chem. Soc. Jpn.*, 1984, **57**, 627.

20 J. C. Bonner and M. E. Fisher, *Phys. Rev. A*, 1964, **135**, 640; M. E. Lines, *J. Phys. Chem. Solids*, 1970, **31**, 101.

21 D. Obertelli, R. H. Friend, D. R. Talham, M. Kurmoo, and P. Day, *Synth. Met.*, 1988, **27**, A375; *J. Phys. Condensed Matter*, 1989, **1**, 5671.

22 M. Lequan, R. M. Lequan, C. Hauw, J. Gaultier, G. Maceno, and P. Delhaes, *Synth. Met.*, 1987, **19**, 409.

23 T. Mori, P. Wang, K. Imaeda, T. Enoki, H. Inokuchi, F. Sakai, and G. Saito, *Synth. Met.*, 1988, **27**, A451.

Received 21*st March* 1989; *Paper* 9/01222B